

Universal transient behavior in large dynamical systems on networks

Wojciech Tarnowski¹, Izaak Neri² and Pierpaolo Vivo²

¹ *Marian Smoluchowski Institute of Physics, Uniwersytet Jagielloński, Krakow (Poland)*

² *Department of Mathematics, King's College London, Strand, London, WC2R 2LS (United Kingdom)*

(Dated: 29 August, 2019)

We develop an exact formalism to study how network architecture influences the transient dynamics of large dynamical systems, described by a set of randomly coupled linear differential equations, in the vicinity of a stationary point. We show that for unidirectional networks the average dynamical response to initial perturbations is universal and only depends on a single parameter, encoding the average interaction strength between the individual constituents. We illustrate our results with numerical simulations of large systems with different types of disorder.

Introduction - Networks of interacting constituents [1, 2] appear in the study of systems as diverse as ecosystems [3–5], neural networks [6–10], financial markets [11–14], signaling networks [15–17] and many others [1, 2, 18]. Traditionally, a strong focus has been put on the issue whether such systems are stable or not at long times [19, 20] because stability is often associated to functionality, e.g., stable ecosystems or economies [21]. However, the short-time transient response to perturbations is less understood despite being of paramount importance for applications: for example, neuroscientists administer magnetic stimulations to the brain and observe different dynamical responses of electrical activity, which are believed to capture different connectivity states of the underlying network of neurons [22]. In many ecological systems, the asymptotic dynamics does not capture the typical time scales accessible in experiments [23–27]. In the context of epidemics, the initial time window before vaccinations become available, makes a crucial difference in limiting the extent of the outbreak [28, 29].

A relevant question is how network architecture determines the early-time dynamics of large systems. For example: (i) how long does a stable system take to return to its stationary state as a function of the network topology and interaction strength among its constituents, and (ii) how long does it take to realize that a seemingly stable system is unstable after all, and disaster is looming? In this Letter we develop an exact formalism based on random matrices and methods from disordered systems to address the early-time behavior of large dynamical systems with sparse topology.

Model setup - Consider N real-valued variables $\zeta_i(t)$, which denote the state of an interacting system at time t . For example, they may represent the abundance of species i in an ecosystem or the activity of the i -th neuron in the brain. We assume that the system evolves according to a system of first-order equations $\partial_t \zeta_i = f_i(\zeta)$, for $i = 1, \dots, N$. Although the functions f_i 's can be arbitrarily complicated, the dynamics can be linearized close to a stationary point ζ^* of the dynamics, such that $f_i(\zeta^*) = 0$, to yield

$$\frac{dy_i(t)}{dt} = \sum_{k=1}^N A_{ik} y_k(t), \quad (1)$$

where the N -dimensional vector $\mathbf{y}(t) = \zeta(t) - \zeta^*$ encodes

deviations from the stationary state, and $A_{ik} = \left(\frac{\partial f_i}{\partial \zeta_k} \right) \Big|_{\zeta^*}$ is the corresponding Jacobian matrix. The spectrum of A – and in particular its eigenvalue with largest real part λ_1 – determines the fate of the system at *large* times: if $\text{Re}[\lambda_1] > 0$, the squared norm $|\mathbf{y}(t)|^2$ diverges exponentially, whereas if $\text{Re}[\lambda_1] < 0$ the stationary state is asymptotically stable and $|\mathbf{y}(t)|^2$ converges to zero. However, the *early-time* dynamics cannot be described in such simple terms and require completely different tools.

To study the early-time dynamics quantitatively, we focus on the response of the squared norm $|\mathbf{y}(t)|^2$ to an initial perturbation \mathbf{y}_0 . To consider *generic* \mathbf{y}_0 , we average $|\mathbf{y}(t)|^2$ over \mathbf{y}_0 , a vector uniformly drawn from the sphere $|\mathbf{y}_0| = \varrho$, where ϱ quantifies the strength of the initial kick. Following [30], the squared norm averaged over \mathbf{y}_0 reads (see [31])

$$\langle |\mathbf{y}(t)|^2 \rangle = \frac{\varrho^2}{N} \text{Tr} e^{A^T t} e^{A t} = \frac{\varrho^2}{N} \sum_{j,k=1}^N e^{t(\lambda_j^* + \lambda_k)} \langle \ell_k | \ell_j \rangle \langle r_j | r_k \rangle, \quad (2)$$

where λ_j 's are the eigenvalues of A , $\langle \ell_k |$ ($|r_k \rangle$) are its left (right) eigenvectors and T denotes the matrix transpose. From (2), one can see that the transient behavior is governed not only by the spectrum of A , but also by the non-orthogonality of its eigenvectors. Indeed, the eigenmodes can interfere constructively resulting in an initial amplification of the signal well before it eventually dies out [32–37]. If A is a normal matrix ($[A, A^T] = 0$) such transient behavior is absent because its eigenvectors are orthogonal [38]. However, non-normal matrices and non-normal networks [39] are prevalent in nature [40] because asymmetry in the interactions is the simplest source of non-normality.

To grasp generic properties of large systems, it is natural to take A as a random matrix of pairwise interactions [5, 19, 41] and further average the squared norm (2) over the disorder $S_N(t) = \langle |\mathbf{y}(t)|^2 \rangle$. This setting has been considered in the literature before for systems with *fully connected* topology [30, 42–45]. There, $S(t) = \lim_{N \rightarrow \infty} S_N(t)$ does not depend on the fine details of the underlying ensemble but only on its spectral radius and thus enjoys a high degree of universality. In the large N limit, and for $A = -\mu \mathbf{1} + X/\sqrt{N}$, with X having independent identically distributed (i.i.d.) entries with

zero mean and finite moments [30, 43], $S(t)$ reads

$$S(t) = \varrho^2 e^{-2\mu t} I_0(2\varrho t), \quad (3)$$

where $\varrho = \max_i |\lambda_i + \mu|$ is the spectral radius of X/\sqrt{N} and $I_0(x)$ is the modified Bessel function of the first kind. From the asymptotics $I_0(x) \sim e^x/\sqrt{2\pi x}$ it follows that the stability of the system is determined by the sign of $\varrho - \mu$.

In order to study how the network architecture affects the dynamics, it is necessary to go beyond the fully connected paradigm. In this Letter, we provide exact formulae for $S(t)$ in cases where A encodes a sparse network structure with prescribed degree distribution as occurring in real systems [1, 46, 47]. The matrix element A_{ij} will then be nonzero only if there is a directed link from node i to node j . We define the neighborhood ∂_j as the set of nodes that are connected to j and $\partial_k \setminus j$ as the neighbourhood of k excluding j .

For sparse random matrices, certain spectral properties are universal, such as the eigenvalues with largest real part [48, 49], while others are strongly model-dependent, such as the spectral distribution [2, 3, 5, 50–52, 55]. While the former dictate the long-time stability of the system, the latter govern the dynamics at finite times, see (2). Therefore, there is no a priori reason to expect universality in the dynamics of networked systems at short times. Surprisingly, as we show in this Letter, for a wide class of large networks the transient dynamics is universally governed by a combination of two relevant parameters. We obtain these results exploiting the cavity method from disordered systems [57–61].

Integral representation - Equation (2) can be recast as [31]

$$\langle |\mathbf{y}(t)|^2 \rangle = \frac{1}{N} \oint_{\gamma} \frac{dz dw}{(2\pi i)^2} e^{t(z+w)} \text{Tr} \frac{1}{z\mathbb{1} - A^T} \frac{1}{w\mathbb{1} - A}, \quad (4)$$

where we have set $\varrho = 1$, and we use a Dunford-Taylor integral [62] over a contour γ enclosing the spectrum of A . The first technical challenge is to rewrite the trace in a form amenable to the cavity method [2, 5]. We recast the trace in terms of the block-trace $\text{bTr} B^{-1}$ as follows

$$\text{Tr} \frac{1}{z\mathbb{1} - A^T} \frac{1}{w\mathbb{1} - A} = -\text{bTr} \begin{pmatrix} \mathbb{0} & w\mathbb{1} - A \\ z\mathbb{1} - A^T & \mathbb{1} \end{pmatrix}^{-1}, \quad (5)$$

where the block-trace bTr of the $2N \times 2N$ matrix B^{-1} on the r.h.s. is equal to $\sum_{j=1}^N [B^{-1}]_{j,j}$, the trace restricted to the upper left block. We can make further progress assuming that A represents a tree graph [63].

Tree structure - In this case, it is useful to reshuffle the entries of the matrix B in (S10) and group them together if they refer to the same node of the original graph described by A . In this way, B becomes a sparse matrix composed of 2×2 blocks and inherits the tree structure of the original graph. This reshuffling allows us to rewrite

$$\text{Tr} \frac{1}{z\mathbb{1} - A^T} \frac{1}{w\mathbb{1} - A} = -\sum_{j=1}^N [\mathbf{G}_j]_{1,1}, \quad (6)$$

in terms of the upper-left corner of 2×2 matrices \mathbf{G}_j ($j = 1, \dots, N$)

$$\mathbf{G}_j = \begin{pmatrix} [B^{-1}]_{j,j} & [B^{-1}]_{j,j+N} \\ [B^{-1}]_{j+N,j} & [B^{-1}]_{j+N,j+N} \end{pmatrix}. \quad (7)$$

To compute \mathbf{G}_j we employ the Schur formula, which for tree structure takes the simplified form [cf. Eq. (62) in [5] or see [31] for more details]

$$\mathbf{G}_j^{-1} = \begin{pmatrix} 0 & w \\ z & 1 \end{pmatrix} - \mathbf{A}_{jj} - \sum_{k \in \partial_j} \mathbf{A}_{jk} \mathbf{G}_k^{(j)} \mathbf{A}_{kj}, \quad (8)$$

where $\mathbf{A}_{jk} = \begin{pmatrix} 0 & A_{jk} \\ A_{kj} & 0 \end{pmatrix}$ and

$$\mathbf{G}_k^{(j)} = \begin{pmatrix} [(B^{(j)})^{-1}]_{k,k} & [(B^{(j)})^{-1}]_{k,k+N} \\ [(B^{(j)})^{-1}]_{k+N,k} & [(B^{(j)})^{-1}]_{k+N,k+N} \end{pmatrix}. \quad (9)$$

The $2(N-1) \times 2(N-1)$ matrix $B^{(j)}$ is obtained by deleting the rows and columns with index j and $j+N$ in B , or equivalently by removing the j -th node from the tree represented by A . The network with the j -th node removed is sometimes called the *cavity graph* [6, 52]. Applying once again the Schur formula on the cavity graph, we obtain the following recursion formula [cf. Eq. (63) in [5]] for $j \in \partial_k$

$$(\mathbf{G}_k^{(j)})^{-1} = \begin{pmatrix} 0 & w \\ z & 1 \end{pmatrix} - \mathbf{A}_{jj} - \sum_{\ell \in \partial_k \setminus j} \mathbf{A}_{k\ell} \mathbf{G}_\ell^{(k)} \mathbf{A}_{\ell k}, \quad (10)$$

which provides a closed system of equations on a tree.

Hereafter, we write matrices A in the form $A_{ij} = C_{ij} J_{ij}$ for $i \neq j$, where $C_{ij} \in \{0, 1\}$ are the entries of the adjacency matrix of the underlying graph and J_{ij} are bond strengths. For $i = j$, we write $A_{ii} = D_i$. Remarkably, the formulas (8) and (10) above simplify for oriented matrices, where the underlying graph consists of unidirectional links such that $C_{ij} C_{ji} = 0$ for $i \neq j$: the last terms on the r.h.s. have off-diagonal entries equal to zero. Therefore,

$$\mathbf{G}_k^{(j)} = \begin{pmatrix} \alpha_k^{(j)} & \frac{1}{z-D_k} \\ \frac{1}{w-D_k} & 0 \end{pmatrix} \quad \mathbf{G}_k = \begin{pmatrix} \alpha_k & \frac{1}{z-D_k} \\ \frac{1}{w-D_k} & 0 \end{pmatrix}, \quad (11)$$

where

$$\alpha_k^{(j)} = \frac{\sum_{\ell \in \partial_k \setminus j} C_{\ell k} \alpha_\ell^{(k)} J_{\ell k}^2 - 1}{(z - D_k)(w - D_k)}, \quad (12)$$

and

$$\alpha_k = \frac{\sum_{\ell \in \partial_k} C_{\ell k} \alpha_\ell^{(k)} J_{\ell k}^2 - 1}{(z - D_k)(w - D_k)}. \quad (13)$$

Comparing the r.h.s. of (12) and (13), we notice that if $C_{jk} = 0$ and $C_{kj} \neq 0$, then $\alpha_k^{(j)} = \alpha_k$. This fact will play a crucial role when performing the disorder average. The equations above could be solved numerically on a fixed instance

of a tree, but to make further analytical progress we consider an ensemble of large random locally tree-like oriented graphs, for which short cycles are rare [1, 4, 65].

Ensemble of locally tree-like oriented matrices - We consider adjacency matrices of weighted oriented random graphs having a prescribed degree distribution $p_{\text{deg}}(k_{\text{in}}, k_{\text{out}}) = p_{\text{deg}}(k_{\text{in}})p_{\text{deg}}(k_{\text{out}})$ with finite second moment. The mean connectivity $c = \sum_{k \geq 0} k p_{\text{deg}}(k)$ is finite and larger than 1 to ensure that the underlying graph has a giant strongly connected component [67]. The bond weights $\{J_{ij}\}$ are taken as i.i.d. random variables with probability density function (pdf) $p_J(x)$ having finite moments, and the diagonal entries D_i are i.i.d. random variables taken from a pdf $p_D(x)$ with compact support.

The spectrum of such matrices in the limit of large N may consist of both continuous and point-like components [5, 68], which may include outliers. As derived in [48, 49], the boundary of the absolutely continuous part is composed of complex λ_b solving

$$r^2 \int dx p_D(x) \frac{1}{|\lambda_b - x|^2} = 1, \quad (14)$$

where $r^2 = c\bar{J}^2$ is the product of the mean connectivity c and the second moment $\bar{J}^2 = \int dx p_J(x)x^2$ of the bond disorder, while the outliers λ_{isol} are the solutions of the equation

$$c\bar{J} \int dx p_D(x) \frac{1}{\lambda_{\text{isol}} - x} = 1 \quad (15)$$

that lie outside the continuous spectrum. Note that (i) outliers are always real, (ii) if $\bar{J} = 0$, there are no outliers, and (iii) while the boundary of the continuous part and the location of outlier(s) are universal, the spectral density inside the boundary is non-universal and depends on the bond disorder [2, 5].

Since the oriented matrices defined in this section are locally tree-like, the cavity formalism developed in the previous section applies. Moreover, we can take the disorder average of the equation (13) over the current ensemble. Given that (i) the variables on the r.h.s. are all statistically independent, and (ii) $\overline{\alpha_k} = \overline{\alpha_\ell^{(k)}} = \bar{\alpha} = [\overline{G_k}]_{1,1}$ for any k, ℓ such that $C_{k\ell} = 1$, as all nodes in the random graph ensemble are statistically equivalent [69], we obtain

$$\bar{\alpha} = (r^2 \bar{\alpha} - 1) \int dx p_D(x) \frac{1}{(z - x)(w - x)}. \quad (16)$$

Solving (16) for $\bar{\alpha}$ and using (4), (6) and (11), we eventually obtain for $S(t) = \lim_{N \rightarrow \infty} S_N(t)$,

$$S(t) = \frac{1}{(2\pi i)^2} \oint_{\gamma} dz dw \frac{e^{t(z+w)}}{\left[\int dx p_D(x) \frac{1}{(z-x)(w-x)} \right]^{-1} - r^2}, \quad (17)$$

which constitutes the main result of this Letter. Remarkably, we see that the transient behavior on oriented graphs is universal: once the diagonal disorder is fixed, everything depends only on the combination $r^2 = c\bar{J}^2$.

It remains to perform the contour integral in (S30) for some specific choice of the diagonal disorder. We present two simple examples with closed-form solutions: (i) fixed diagonal, $p_D(x) = \delta(x + \mu)$ and (ii) bimodal disorder, $p_D(x) = (1 - q)\delta(x + \mu_1) + q\delta(x + \mu_2)$.

Case (i) - In this case, the integral (S30) can be performed using residues. Changing variables $z' = z + \mu$ and $w' = w + \mu$, we obtain

$$S(t) = \frac{1}{2\pi i} e^{-2\mu t} \oint_{\gamma'} dz' \frac{e^{t(z' + r^2/z')}}{z'} = e^{-2\mu t} I_0(2rt). \quad (18)$$

Quite remarkably, Eq. (18) for sparse oriented graphs and Eq. (3) for fully connected structures share the same functional form, and therefore the two models fall into the same universality class. Indeed, if $\bar{J} = 0$, then r is precisely the spectral radius ρ of A (see (14)). Notice that for large t ,

$$S(t) \sim \frac{1}{\sqrt{4\pi r t}} e^{2t(r - \mu)}, \quad (19)$$

where the exponent in (19) is in fact equal to $2t \max \text{Re}[\lambda_b]$ (see Eq. (14)).

In Fig. 1 (top row), we illustrate our findings with numerical simulations on oriented graphs with different $p_J(x)$, all sharing the same non-zero \bar{J} . We observe three qualitatively different scenarios: (a) the system is both transiently and asymptotically stable ($\text{Re}[\lambda_b] < 0$ and $\lambda_{\text{isol}} < 0$), (b) the system is transiently stable but asymptotically unstable ($\text{Re}[\lambda_b] < 0$ and $\lambda_{\text{isol}} > 0$), and (c) the system is unstable ($\max \text{Re}[\lambda_b] > 0$).

We remark that the theory in Eq. (S30) is obtained by taking the limit $N \rightarrow \infty$ at *fixed* time, while in the simulations we work with a fixed system size N and look at its time evolution. As a result, there will be a crossover time $t^*(N)$ — which diverges with N — after which the theory and simulations are expected to diverge. We clearly see this effect in cases (b) and (c) of Fig. 1.

More specifically, for $t \gg t^*(N)$, the contribution from the eigenmode with largest real part $\sim a_N e^{2t \text{Re}[\lambda_1]}$ (where a_N is independent of t and vanishes for large N) will dominate the sum in Eq. (2) in every single realization of the $N \times N$ numerical experiment. For instance, in case (b) the location of the positive outlier will always make the system eventually unstable for any finite N however large. This behavior is not captured by our formula (S30), where the limit $N \rightarrow \infty$ is taken *before* $t \rightarrow \infty$, making a_N vanish immediately. Instead in case (c) the leading asymptotics $\sim a_N e^{2t \text{Re}[\lambda_1]}$ should be contrasted with Eq. (19): while the exponential behavior is perfectly captured by our formula, the difference in prefactors (a_N vs. $\sim 1/\sqrt{t}$) will materialize at sufficiently large t leading to the observed discrepancy. For $t < t^*(N)$, we observe perfect agreement between theory and simulations, proving that the precise connectivity structure and the type of bond disorder do not matter, and only the combination $r^2 = c\bar{J}^2$ plays a role, as predicted by the theory. In case (a), theory and simulations are in perfect agreement at all times, and $1/(2(r - \mu))$ provides the typical relaxation time to stationarity.

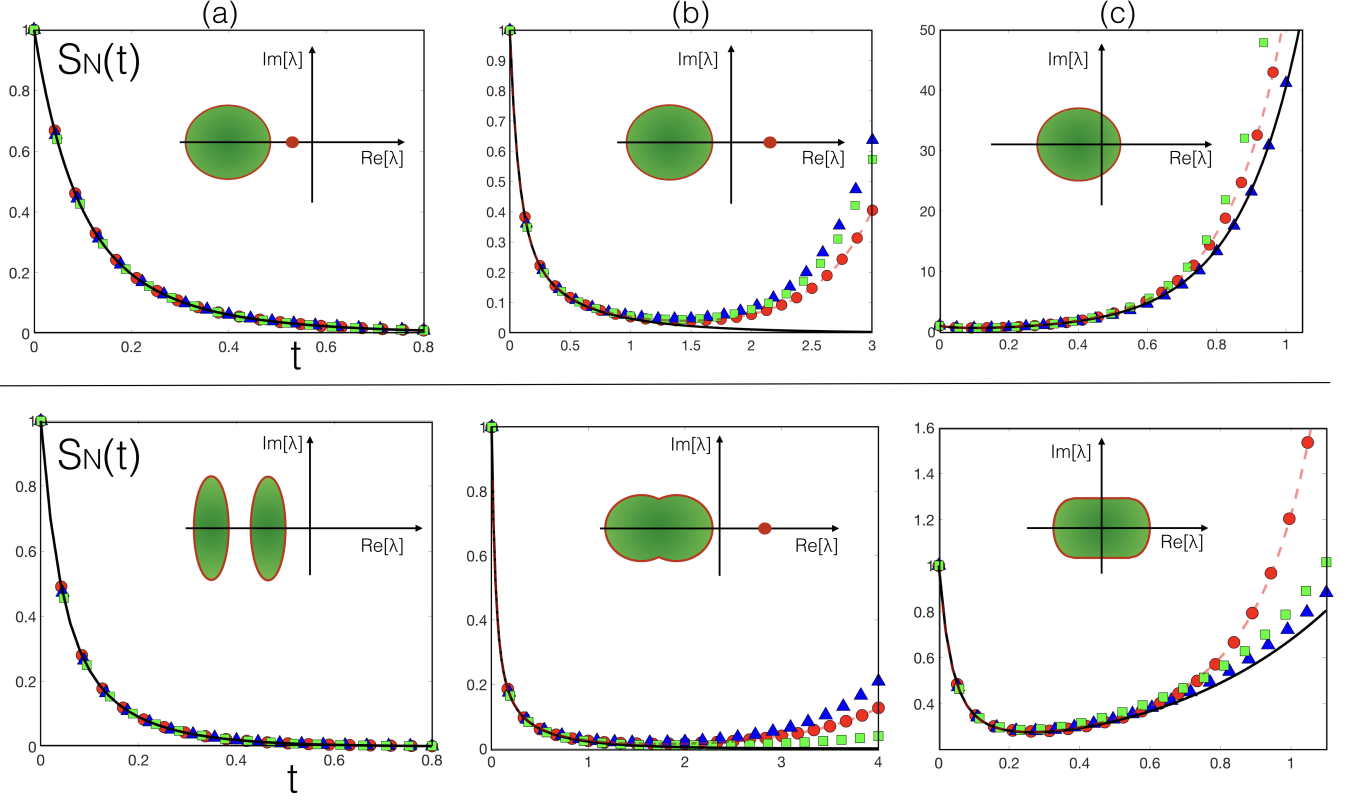


FIG. 1: $S_N(t)$ for weighted oriented graphs with Poissonian connectivity with mean degree $c = 2$, with fixed diagonal (Top Row) and bimodal diagonal disorder (Bottom Row). The theoretical result for $S(t)$ is provided in black solid line (see Eqs. (18) and (21), respectively). Symbols denote numerical solution of the differential equation (1) for $N = 5000$, averaged over 25 initial conditions and 5 realizations of the underlying graph. Red circles stand for Gaussian bond disorder, blue triangles for uniform bond disorder, and green squares for Laplace-distributed disorder. The parameters for different panels are described below. We show schematically in the insets the location of the continuous part of the spectrum and the outlier (if present), according to formulae (14) and (15). **Top row:** Fixed diagonal at $-\mu = -5$. (a) $\bar{J} = 2$ and $\bar{J}^2 = 5$, (b) $\bar{J} = 3$ and $\bar{J}^2 = 10$, and (c) $\bar{J} = 4$ and $\bar{J}^2 = 32$. In panels (b) and (c), the red dashed curves represent Eq. (20) with fitted values of parameters $a = 7.7 \cdot 10^{-4}$, $b = 1.04$ and $a = 4.2 \cdot 10^{-3}$, $b = 4.03$, respectively. Eqs. (14) and (15) simplify in this case as $r^2 = c\bar{J}^2 = |\lambda_b - \mu|^2$ and $\lambda_{\text{isol}} = c\bar{J} - \mu$. **Bottom row:** Diagonal entries taken at random between $-\mu_1 = -5$ and $-\mu_2 = -14$ with equal probability ($q = 1/2$). (a) $\bar{J} = 2$ and $\bar{J}^2 = 5$, (b) $\bar{J} = 4$ and $\bar{J}^2 = 17$, and (c) $\bar{J} = 4$ and $\bar{J}^2 = 32$. In panels (b) and (c), the red dashed curves represent Eq. (20) with fitted values of parameters $a = 1.1 \cdot 10^{-3}$, $b = 0.6$ and $a = 1.8 \cdot 10^{-4}$, $b = 4.0$, respectively.

In order to capture both the transient and asymptotic behaviors, we can modify $S(t)$ by including the effect of the largest eigemode as

$$\tilde{S}(t) = S(t) + ae^{2bt}, \quad (20)$$

where a and b are two (albeit non-universal) fitting parameters. This is illustrated in Fig. 1 (b) and (c). We observe empirically that universality is broken after $t^*(N)$. Note that in the panel (b) the fitted exponent $b \approx \lambda_{\text{isol}}$, therefore the fit captures both the early-time and the asymptotic regimes. However, in panel (c) the exponent b is different from $\max \text{Re}[\lambda_b]$ because the asymptotic regime is reached at much larger times than plotted. This discrepancy stems from the fact that the spectral gap in (b) is finite whereas it tends to 0 as $N \rightarrow \infty$ in (c).

Case (ii) - In the case of bimodal disorder, one can evaluate the integral in Eq. (S30) using residues after employing

a geometric series representation of the integrand to get (see Supplemental Material [31])

$$S(t) = (1 - q)e^{-2\mu_1 t} I_0(2rt\sqrt{1 - q}) + qe^{-2\mu_2 t} I_0(2rt\sqrt{q}) + e^{-2\mu_1 t} \Psi(t), \quad (21)$$

where

$$\Psi(t) = \sum_{m \geq 1} \frac{(rt)^{2m}}{(m!)^2} \sum_{n=1}^m \binom{m+1}{n} q^n (1 - q)^{m-n+1} \times [{}_1F_1(n; m+1; -(\mu_2 - \mu_1)t)]^2, \quad (22)$$

in terms of a confluent hypergeometric function ${}_1F_1$. It is interesting to notice that $S(t)$ can be split into three contributions, which have an appealing dynamical interpretation. The system consists of two sub-populations associated with relaxation rates μ_1 and μ_2 . Neglecting interactions between them,

each of these two sub-populations would evolve in isolation according to Eq. (18), albeit with reduced connectivities qc and $(1-q)c$, respectively. The first two terms in (21) describe precisely the dynamics of these two isolated populations. The third term instead describes their dynamical interference due to coupling. In Fig. 1 (bottom row), we compare the theoretical formula (21) with numerical simulations, and observe a qualitatively very similar scenario as previously discussed for the case of fixed diagonal. In particular, the dynamics is universal up to time $t^*(N)$ for cases (b) and (c), and then theory and simulations diverge in a non-universal fashion. In contrast, for case (a) the agreement is perfect at all times.

Discussion - We have shown how the underlying network architecture affects the response of a dynamical system to initial perturbations, and found that for systems with unidirectional interactions the short-time dynamics encoded in $S(t)$ only depends on the single combination $r^2 = cJ^2$ and on the diagonal disorder. Therefore, it is not possible to conclude anything about the fate of the system at large times by observing $|y(t)|^2$ only up to time $t^*(N)$. It would be interesting to explore how far this universality extends to other observables such as higher order moments and full distributions.

As a final outlook, we remark that our theory also applies to non-oriented graph, but it would be more challenging to derive as explicit results. The cavity method has also been extended to the case of networks with small cycles [71–75] and it would be interesting to extend this formalism to these cases as well.

Acknowledgments - WT is supported by ETIUDA scholarship 2018/28/T/ST1/00470 from National Science Center and the Diamond Grant 0225/DIA/2015/44 from the Polish Ministry of Science and Higher Education. WT is grateful to King's College London for hospitality, where this work was done.

-
- [1] M. Newman, *Networks: an introduction*, Oxford University Press (2010).
 - [2] S. N. Dorogovtsev and J. F. F. Mendes, *Evolution of networks: From biological nets to the Internet and WWW*, Oxford University Press (2013).
 - [3] J. Bascompte and P. Jordano, *Plant-animal mutualistic networks: the architecture of biodiversity*, *Annu. Rev. Ecol. Evol. Syst.* **38**, 567-593 (2007).
 - [4] T. C. Ings, et al., *Ecological networks beyond food webs*, *Journal of Animal Ecology* **78**, 253-269 (2009).
 - [5] S. Allesina and S. Tang, *The stability-complexity relationship at age 40: a random matrix perspective*, *Population Ecology* **57**, 63 (2015).
 - [6] H. Sompolinsky, A. Crisanti and H.-J. Sommers, *Chaos in random neural networks*, *Phys. Rev. Lett.* **61**, 259 (1988).
 - [7] O. Sporns, D. R. Chialvo, M. Kaiser and C. C. Hilgetag, *Organization, development and function of complex brain networks*, *Trends Cogn. Sci.* **8**, 418 (2004).
 - [8] A. C. C. Coolen, R. Kühn and P. Sollich, *Theory of Neural Information Processing Systems*, Oxford University Press (2005).
 - [9] N. Brunel, *Dynamics of sparsely connected networks of excitatory and inhibitory spiking neurons*, *Journal of computational neuroscience* **8**, 183-208 (2000).
 - [10] E. Bullmore and O. Sporns, *Complex brain networks: graph theoretical analysis of structural and functional systems*, *Nature Reviews Neuroscience* **10**, 186 (2009).
 - [11] F. Allen and A. Babus, *Networks in Finance* (2008). Wharton Financial Institutions Center Working Paper No. 08-07. Available at SSRN: <https://ssrn.com/abstract=1094883>.
 - [12] A. G. Haldane and R. M. May, *Systemic risk in banking ecosystems*, *Nature* **469**, 351 (2011).
 - [13] M. Bardoscia, S. Battiston, F. Caccioli and G. Caldarelli, *Pathways towards instability in financial networks*, *Nature Communications* **8**, 14416 (2017).
 - [14] F. Caccioli, P. Barucca and T. Kobayashi, *Network models of financial systemic risk: A review*, *Journal of Computational Social Science* **1**, 81 (2018).
 - [15] J. D. Jordan, E. M. Landau and R. Iyengar, *Signaling networks: the origins of cellular multitasking*, *Cell* **103**, 193 (2000).
 - [16] U. Alon, *An introduction to systems biology: design principles of biological circuits*, Chapman and Hall/CRC (2006).
 - [17] C. Hens, U. Harush, S. Haber, R. Cohen and B. Barzel, *Spatiotemporal signal propagation in complex networks*, *Nature Physics* **15**, 403412 (2019).
 - [18] G. Cimini, T. Squartini, F. Saracco, D. Garlaschelli, A. Gabrielli and G. Caldarelli, *The statistical physics of real-world networks*, *Nature Reviews Physics* **1**, 58 (2019).
 - [19] R. M. May, *Will a large complex system be stable?*, *Nature* **238**, 413 (1972).
 - [20] S. Allesina and S. Tang, *Stability criteria for complex ecosystems*, *Nature* **483**, 205 (2012).
 - [21] J. Moran and J.-P. Bouchaud, *Will a Large Economy Be Stable?*, Preprint arXiv:1901.09629 (2019).
 - [22] M. Massimini, F. Ferrarelli, R. Huber, S. K. Esser, H. Singh and G. Tononi, *Breakdown of cortical effective connectivity during sleep*, *Science* **309**, 2228 (2005).
 - [23] M. G. Neubert and H. Caswell, *Alternatives to resilience for measuring the responses of ecological systems to perturbations*, *Ecology* **78**, 653-665 (1997).
 - [24] A. Hastings, *Transients: the key to long-term ecological understanding?*, *Trends in Ecology & Evolution* **19**, 39-45 (2004).
 - [25] D. N. Koons, J. B. Grand, B. Zinner and R. F. Rockwell, *Transient population dynamics: relations to life history and initial population state*, *Ecological Modelling* **185**, 283-297 (2005).
 - [26] S. Tang and S. Allesina, *Reactivity and stability of large ecosystems*, *Frontiers in Ecology and Evolution* **2**, 21 (2014).
 - [27] J. F. Arnoldi, A. Bideault, M. Loreau and B. Haegeman, *How ecosystems recover from pulse perturbations: A theory of short-to long-term responses*, *Journal of Theoretical Biology* **436**, 79-92 (2018).
 - [28] R. Pastor-Satorras, C. Castellano, P. Van Mieghem and A. Vespignani, *Epidemic processes in complex networks*, *Reviews of Modern Physics* **87**, 925 (2015).
 - [29] C.-H. Lee, S. Tenneti and D. Y. Eun, *Transient Dynamics of Epidemic Spreading and its Mitigation on Large Networks*, Preprint arXiv:1903.00167 (2019).
 - [30] B. Mehlhag and J. T. Chalker, *Statistical properties of eigenvectors in non-Hermitian Gaussian random matrix ensembles*, *J. Math. Phys.* **41**, 3233 (2000).
 - [31] See Supplemental Material for a derivation of the two formulas (2) and (4), the cavity equations (8) and (10) and the explicit expression (21)-(22) $S(t)$ in the case of bimodal disorder.
 - [32] L. Ridolfi, C. Camporeale, P. D'Odorico and F. Laio, *Transient growth induces unexpected deterministic spatial patterns in the Turing process*, *Europhys. Lett.* **95**, 18003 (2011).
 - [33] B. K. Murphy and K. D. Miller, *Balanced Amplification: A*

- New Mechanism of Selective Amplification of Neural Activity Patterns*, *Neuron* **61**, 635 (2009).
- [34] G. Hennequin, T. P. Vogels and W. Gerstner, *Optimal control of transient dynamics in balanced networks supports generation of complex movements*, *Neuron* **82**, 1394 (2014).
- [35] F. Caravelli and P. P. A. Staniczenko, *Bounds on Transient Instability for Complex Ecosystems*, *PLoS ONE* **11**(6), e0157876 (2016).
- [36] E. Gudowska-Nowak, M. A. Nowak, D. R. Chialvo, J. K. Ochoa and W. Tarnowski, *From synaptic interactions to collective dynamics in random neural networks models: critical role of eigenvector and transient behavior*, Preprint arXiv:1805.03592 (2018).
- [37] D. V. Savin and V. V. Sokolov, *Quantum versus classical decay laws in open chaotic systems*, *Phys. Rev. E* **56**, R4911(R) (1998).
- [38] L. N. Trefethen and M. Embree, *Spectra and pseudospectra: the behavior of nonnormal matrices and operators*, Princeton University Press (2005).
- [39] M. Asllani and T. Carletti, *Topological resilience in non-normal networked systems*, *Phys. Rev. E* **97**, 042302 (2018).
- [40] M. Asllani, R. Lambiotte and T. Carletti, *Structure and dynamical behavior of non-normal networks*, *Science Advances* **4** (12), eaau9403 (2018).
- [41] Y. V. Fyodorov and B. A. Khoruzhenko, *Nonlinear analogue of the May-Wigner instability transition*, *PNAS* **113**, 6827 (2016).
- [42] J. Grela, *What drives transient behavior in complex systems?*, *Phys. Rev. E* **96**, 022316 (2017).
- [43] L. Erdős, T. Krüger and D. Renfrew, *Power law decay for systems of randomly coupled differential equations*, *SIAM J. Math. Anal.* **50**, 3271 (2018).
- [44] D. Martí, N. Brunel, and S. Ostojic, *Correlations between synapses in pairs of neurons slow down dynamics in randomly connected neural networks*, *Phys. Rev. E* **97**, 062314 (2018).
- [45] L. Erdős, T. Krüger and D. Renfrew, *Randomly coupled differential equations with correlations*, arXiv:1908.05178 (2019).
- [46] A. Clauset, C. R. Shalizi and M. E. J. Newman, *Power-law distributions in empirical data*, *SIAM review* **51**, 661-703 (2009).
- [47] S. N. Dorogovtsev, A. V. Goltsev, and J. F. F. Mendes, *Critical phenomena in complex networks*, *Rev. Mod. Phys.* **80**, 1275 (2008).
- [48] I. Neri and F. L. Metz, *Eigenvalue outliers of non-hermitian random matrices with a local tree structure*, *Phys. Rev. Lett.* **117**, 224101 (2016).
- [49] I. Neri and F. L. Metz, *Spectral theory for the stability of dynamical systems on large oriented locally tree-like graphs.*, arXiv:1908.07092, (2019)
- [50] G. J. Rodgers and A. J. Bray, *Density of states of a sparse random matrix*, *Phys. Rev. B* **37**, 3557 (1988).
- [51] R. Kühn, *Spectra of sparse random matrices*, *J. Phys. A: Math. Theor.* **41**, 295002 (2008).
- [52] T. Rogers, K. Takeda, I. Pérez Castillo and R. Kühn, *Cavity approach to the spectral density of sparse symmetric random matrices*, *Phys. Rev. E* **78**, 031116 (2008).
- [53] T. Rogers and I. Pérez Castillo, *Cavity approach to the spectral density of non-Hermitian sparse matrices*, *Phys. Rev. E* **79**, 012101 (2009).
- [54] I. Neri and F. L. Metz, *Spectra of sparse non-hermitian random matrices: An analytical solution*, *Phys. Rev. Lett.* **109**, 030602 (2012).
- [55] S. Allesina, J. Grilli, G. Barabás, S. Tang, J. Aljadeff and A. Maritan, *Predicting the stability of large structured food webs*, *Nature Communications* **6**, 7842 (2015).
- [56] F. L. Metz, I. Neri and T. Rogers, *Spectral Theory of Sparse Non-Hermitian Random Matrices*, Preprint arXiv:1811.10416 - to appear in *J. Phys. A: Math. Theor.* (2019).
- [57] R. Abou-Chacra, D. J. Thouless and P. W. Anderson, *A self-consistent theory of localization*, *J. Phys. C: Solid State Phys.* **6**, 1734 (1973).
- [58] M. Mézard, G. Parisi and M. Virasoro, *Spin glass theory and beyond: An introduction to the replica method and its applications*, Vol. 9. World Scientific Publishing Company (1987).
- [59] Y. Weiss and W. T. Freeman, *Correctness of belief propagation in Gaussian graphical models of arbitrary topology*, *Neural Comput.* **13**, 2173 (2001).
- [60] M. Mézard and G. Parisi, *The Bethe lattice spin glass revisited*, *Eur. Phys. J. B* **20**, 217-233 (2001).
- [61] F. Zamponi, Preprint arXiv:1008.4844v5 (2014).
- [62] R. A. Horn and C. R. Johnson, *Matrix Analysis*, 2nd Ed., Cambridge University Press (2012).
- [63] B. Bollobás, *Modern graph theory*, Vol. 184. Springer Science & Business Media (2013).
- [64] M. Mézard and G. Parisi, *The cavity method at zero temperature*, *Journal of Statistical Physics* **111**, 1-34 (2003).
- [65] A. Dembo and A. Montanari, *Ising models on locally tree-like graphs*, *The Annals of Applied Probability* **20**, 565-592 (2010).
- [66] C. Bordenave and M. Lelarge, *Resolvent of large random graphs*, *Random Struct. Alg.* **37**, 332 (2010).
- [67] S. N. Dorogovtsev, J. F. F. Mendes and A. N. Samukhin, *Giant strongly connected component of directed networks*, *Phys. Rev. E* **64**, 025101 (2001).
- [68] M. Reed and B. Simon, *Methods of Modern Mathematical Physics: Functional Analysis*, Academic Press Inc. (1972).
- [69] D. Aldous and J.M. Steele, *The objective method: probabilistic combinatorial optimization and local weak convergence*, Springer Verlag, 2003, pp. 172. Probability on discrete structures (H.Kesten, ed.), (Springer Verlag, Heidelberg, 2003), pp.1-72.
- [70] W. Tarnowski, I. Neri and P. Vivo, *Cavity approach to the transient dynamics of networked systems*, in preparation.
- [71] F. L. Metz, I. Neri and D. Bollé, *Spectra of sparse regular graphs with loops*, *Phys. Rev. E* **84**, 055101 (2011).
- [72] D. Bollé, F. L. Metz and I. Neri, *On the spectra of large sparse graphs with cycles*, *Spectral Analysis, Differential Equations and Mathematical Physics: A Festschrift in Honor of Fritz Gesztesy's 60th Birthday*, H. Holden et al. (eds), Proceedings of Symposia in Pure Mathematics, vol. 87, Amer. Math. Soc., pp. 35-58 (2013).
- [73] A. C. C. Coolen, *Replica methods for loopy sparse random graphs*, *J. Phys.: Conf. Ser.* **699**, 012022 (2016).
- [74] M. E. J. Newman, *Spectra of networks containing short loops* Preprint arXiv:1902.04595 (2019).
- [75] P.V. Aceituno, T. Rogers, and H. Schomerus, *Universal hypotrochoidic law for random matrices with cyclic correlations*, *Physical Review E* **100**, 010302 (2019).

Supplemental Material for “Universal transient behavior in large dynamical systems on networks”

Wojciech Tarnowski¹, Izaak Neri² and Pierpaolo Vivo²

¹ Marian Smoluchowski Institute of Physics, Uniwersytet Jagielloński, Krakow (Poland)

² Department of Mathematics, King’s College London, Strand, London, WC2R 2LS (United Kingdom)

This document provides additional information on the manuscript “Universal transient behavior in large dynamical systems on networks”.

In the first section we derive the formula for the averaged squared norm $\langle |\mathbf{y}(t)|^2 \rangle$. In the second section we derive the integral formula (4). In the third section we derive the cavity equations (8) and (10). In the final fourth section, we derive the formulae (21) and (22).

Although the calculations presented in the first two sections have appeared before in the literature, we present them here in order to keep the paper self-contained.

DERIVATION OF FORMULA FOR $\langle |\mathbf{y}(t)|^2 \rangle$

Using the fact that the vector $\mathbf{y}(t)$ solving Eq. (1) is of the form

$$\mathbf{y}(t) = e^{At} \mathbf{y}(0), \quad (\text{S1})$$

we have a general expression for the squared norm

$$|\mathbf{y}(t)|^2 = \mathbf{y}^T(0) e^{A^T t} e^{At} \mathbf{y}(0). \quad (\text{S2})$$

We observe that any initial condition can be generated by choosing a single representative \mathbf{y}_0 taken from a N -dimensional sphere $|\mathbf{y}_0|^2 = \varrho^2$ and acting by a matrix from the orthogonal group $O(N)$ (the group of isometries of the N -sphere), $\mathbf{y}(0) = O\mathbf{y}_0$. Averaging (S2) over initial conditions is therefore equivalent to taking the average of the following expression

$$\mathbf{y}_0^T O^T e^{A^T t} e^{At} O \mathbf{y}_0 \quad (\text{S3})$$

with respect to the uniform (Haar) measure on the orthogonal group. In the next step we use [1]

$$\langle O_{ij} O_{kl} \rangle = \frac{1}{N} \delta_{ik} \delta_{jl}, \quad (\text{S4})$$

which directly leads to the first equality in Eq. (2)

$$\langle |\mathbf{y}(t)|^2 \rangle = \frac{|\mathbf{y}(0)|^2}{N} \text{Tr} e^{A^T t} e^{At}. \quad (\text{S5})$$

The second equality follows from the spectral decomposition $A = \sum_{k=1}^N |r_k\rangle \lambda_k \langle l_k|$ applied to the matrix exponential and the cyclicity of the trace.

DERIVATION OF THE INTEGRAL FORMULA (4)

We use Cauchy’s integral formula

$$\frac{1}{(2\pi i)} \oint_{\gamma} \frac{f(z)}{z - a} dz = f(a), \quad (\text{S6})$$

which holds for any analytic function f and any closed counterclockwise-oriented contour γ in the complex plane which encompasses a region that contains the point a in its interior. Applying Cauchy’s integral formula to (2) we obtain

$$\langle |\mathbf{y}(t)|^2 \rangle = \frac{\varrho^2}{N} \oint_{\gamma} \oint_{\gamma} \frac{dz dw}{(2\pi i)^2} \sum_{j=1}^N \sum_{k=1}^N e^{t(z+w)} \frac{\langle l_k | l_j \rangle \langle r_j | r_k \rangle}{(w - \lambda_k)(z - \lambda_j^*)} \quad (\text{S7})$$

with a contour γ encompassing all the eigenvalues λ_j of A .

Using the spectral decompositions

$$\sum_{j=1}^N \frac{|l_j\rangle\langle r_j|}{z - \lambda_j^*} = \frac{1}{z\mathbb{1} - A^T}, \quad \sum_{k=1}^N \frac{|r_k\rangle\langle l_k|}{w - \lambda_k} = \frac{1}{w\mathbb{1} - A}, \quad (\text{S8})$$

one can see that the relation (S7) implies (4).

DERIVATION OF THE CAVITY EQUATIONS (8) AND (10)

We use the formalism in [2–5].

The first step is Eq. (5), namely,

$$\text{Tr} \frac{1}{z\mathbb{1} - A^T} \frac{1}{w\mathbb{1} - A} = -\text{bTr}_{11} B^{-1} \quad (\text{S9})$$

where

$$B = \begin{pmatrix} 0 & w\mathbb{1} - A \\ z\mathbb{1} - A^T & \mathbb{1} \end{pmatrix}, \quad (\text{S10})$$

and the block-trace bTr_{11} of a $2N \times 2N$ matrix X is equal to $\sum_{j=1}^N [X]_{j,j}$, the trace restricted to the upper left block.

The matrix B can be seen as a replicated version of the original matrix A , where each node of the original graph has two replicas, one with label i and the other with label $i + N$ ($i = 1, \dots, N$), which are located therefore far apart in the matrix B . We now want to create a new matrix that preserves the same connectivity structure of the original matrix (encoded in C), which is achieved by bundling together labels that refer to the same node.

To this end we permute the rows and columns of the matrix B . The permutation we perform defines the matrix \tilde{B} , whose entries are assigned according to the following operations:

$$B_{i,j} \rightarrow \begin{cases} \tilde{B}_{2i-1, 2j-1} & \text{if } 1 \leq i, j \leq N \\ \tilde{B}_{2(i-N), 2j-1} & \text{if } N+1 \leq i \leq 2N, 1 \leq j \leq N \\ \tilde{B}_{2i-1, 2(j-N)} & \text{if } 1 \leq i \leq N, N+1 \leq j \leq 2N \\ \tilde{B}_{2(i-N), 2(j-N)} & \text{if } N+1 \leq i, j \leq 2N. \end{cases} \quad (\text{S11})$$

This permutation is performed by conjugating the matrix B as PBP , where P is a suitably defined permutation matrix.

We then obtain the permuted matrix \tilde{B} which consists of diagonal 2×2 blocks

$$\tilde{B}_{ii} = \begin{pmatrix} 0 & w - A_{ii} \\ z - A_{ii} & 1 \end{pmatrix} := \begin{pmatrix} 0 & w \\ z & 1 \end{pmatrix} - A_{ii}, \quad (\text{S12})$$

and off-diagonal blocks of the form

$$\tilde{B}_{ij} = \begin{pmatrix} 0 & -A_{ij} \\ -A_{ji} & 0 \end{pmatrix} := -A_{ij}, \quad (\text{S13})$$

for $i, j = 1, \dots, N$. Note that now the matrix \tilde{B} is a block matrix (formed by 2×2 blocks) that has the same connectivity structure as the matrix A .

The elements of B^{-1} , which we need in Eq. (S9), are related to the elements of \tilde{B}^{-1} in the following way:

$$\tilde{B}^{-1} = (PBP)^{-1} \Rightarrow P\tilde{B}^{-1}P = B^{-1}, \quad (\text{S14})$$

since a permutation matrix is an orthogonal transformation. Moreover,

$$\begin{aligned} \text{bTr}_{11} B^{-1} &= \text{bTr}_{11} [P\tilde{B}^{-1}P] = \\ &= \sum_{j=1}^N [P\tilde{B}^{-1}P]_{j,j} = \sum_{j=1}^N [\tilde{B}^{-1}]_{2j-1, 2j-1}, \end{aligned} \quad (\text{S15})$$

where in the first line we used Eq. (S14), and in the second line the fact that the permutation matrix P maps indices j into $2j - 1$ if $1 \leq j \leq N$.

Therefore, the objects of interest are now the elements $[\tilde{B}^{-1}]_{2j-1, 2j-1}$ of the inverse matrix of \tilde{B} . We first define the 2×2 matrices G_j for $j = 1, \dots, N$ as

$$G_j = \begin{pmatrix} [G_j]_{1,1} & [G_j]_{1,2} \\ [G_j]_{2,1} & [G_j]_{2,2} \end{pmatrix} = \begin{pmatrix} [\tilde{B}^{-1}]_{2j-1, 2j-1} & [\tilde{B}^{-1}]_{2j-1, 2j} \\ [\tilde{B}^{-1}]_{2j, 2j-1} & [\tilde{B}^{-1}]_{2j, 2j} \end{pmatrix}, \quad (\text{S16})$$

which implies from Eq. (S15) that

$$\text{Tr} \frac{1}{z\mathbb{1} - A^T} \frac{1}{w\mathbb{1} - A} = -b \text{Tr}_{11} B^{-1} = - \sum_{j=1}^N [G_j]_{1,1}. \quad (\text{S17})$$

Note that the one-point resolvent can also be recovered from this formalism as

$$\frac{1}{N} \text{Tr} \left[\frac{1}{z\mathbb{1} - A^T} \right] = -\frac{1}{N} \sum_{j=1}^N [G_j]_{2,1} \quad (\text{S18})$$

and

$$\frac{1}{N} \text{Tr} \left[\frac{1}{w\mathbb{1} - A} \right] = -\frac{1}{N} \sum_{j=1}^N [G_j]_{1,2}. \quad (\text{S19})$$

Up to now, the discussion has not made any assumptions on the connectivity structure of the adjacency matrix C . To proceed further, we now assume that C (and therefore \tilde{B}) has the connectivity of a tree, which means that there are no cycles.

In order to find an equation for the G_j , we will use the *Schur inversion formula*

$$\begin{pmatrix} \mathbf{a} & \mathbf{b} \\ \mathbf{c} & \mathbf{d} \end{pmatrix}^{-1} = \begin{pmatrix} \mathbf{s}_d & -\mathbf{s}_d \mathbf{b} \mathbf{d}^{-1} \\ -\mathbf{d}^{-1} \mathbf{c} \mathbf{s}_d & \mathbf{s}_a \end{pmatrix}, \quad (\text{S20})$$

with $\mathbf{s}_d = (\mathbf{a} - \mathbf{b} \mathbf{d}^{-1} \mathbf{c})^{-1}$ the inverse of the Schur complement of \mathbf{d} and $\mathbf{s}_a = (\mathbf{d} - \mathbf{c} \mathbf{a}^{-1} \mathbf{b})^{-1}$ the inverse of the Schur complement of \mathbf{a} . We illustrate how this works for $j = 1$ and later generalize for arbitrary j .

In order to implement the Schur inversion formula, we represent \tilde{B} with the block matrix structure of the form

$$\tilde{B} = \begin{pmatrix} \tilde{B}_{11} & \tilde{B}_{1\star} \\ \tilde{B}_{\star 1} & \tilde{B}^{(1)} \end{pmatrix}, \quad (\text{S21})$$

where \tilde{B}_{11} is the 2×2 matrix defined in Eq. (S12), $\tilde{B}_{1\star}$ and $\tilde{B}_{\star 1}$ are $2 \times 2(N-1)$ and $2(N-1) \times 2$ matrices respectively, and $\tilde{B}^{(1)}$ is a $2(N-1) \times 2(N-1)$ matrix. Note that $\tilde{B}^{(1)}$ is the \tilde{B} matrix corresponding to the forest, consisting of $|\partial_1|$ isolated trees, which is obtained by removing node 1 from the original tree. In the field of disordered systems, this is referred to as the *cavity graph* corresponding to node 1 [6].

Now, we are ready to find an equation for G_1 , the upper-left 2×2 block of \tilde{B}^{-1} (see Eq. (S16)), taking full advantage of the block structure in Eq. (S21). The Schur formula applied to the upper-left 2×2 block of \tilde{B} gives the following

$$G_1 = \frac{1}{\tilde{B}_{11} - \tilde{B}_{1\star} [\tilde{B}^{(1)}]^{-1} \tilde{B}_{\star 1}}. \quad (\text{S22})$$

Now, using Eq. (S12) and the fact that both $\tilde{B}_{1\star}$ and $\tilde{B}_{\star 1}$ are concatenations of matrices of the form A (see Eq. (S13)), we obtain

$$G_1 = \frac{1}{\begin{pmatrix} 0 & w \\ z & 1 \end{pmatrix} - A_{11} - \sum_{k \in \partial_1} \sum_{\ell \in \partial_1} A_{1k} G_{k\ell}^{(1)} A_{\ell 1}}, \quad (\text{S23})$$

where

$$G_{k\ell}^{(1)} = \begin{pmatrix} [(\tilde{B}^{(1)})^{-1}]_{2k-1, 2\ell-1} & [(\tilde{B}^{(1)})^{-1}]_{2k-1, 2\ell} \\ [(\tilde{B}^{(1)})^{-1}]_{2k, 2\ell-1} & [(\tilde{B}^{(1)})^{-1}]_{2k, 2\ell} \end{pmatrix}. \quad (\text{S24})$$

For simplicity we call $G_k^{(1)} = G_{kk}^{(1)}$. In the sums in Eq. (S23), we omit contributions from $k, \ell \notin \partial_1$ because A_{1k} and $A_{\ell 1}$ are null matrices in this case (see Eq. (S13)).

Now, if $k \neq \ell$ and $k, \ell \in \partial_1$, then k and ℓ belong to isolated trees in the cavity graph and therefore the matrices $G_{k\ell}^{(1)}$ are null. Indeed, \tilde{B}^{-1} has the mathematical form of a resolvent matrix $(u\mathbf{1} - X)^{-1}$ where X is a block matrix built out of 2×2 matrices located at the edges of the graph represented by A . Expanding $(u\mathbf{1} - X)^{-1} = \sum_{n=0}^{\infty} X^n / u^{n+1}$ we notice that $[(u\mathbf{1} - X)^{-1}]_{k\ell} = 0$ if k and ℓ belong to isolated trees. Indeed, this follows from the fact that $[X^n]_{k\ell}$ denotes the sum of the weights of the paths in the graph of length n that connect node k to node ℓ . If there exists no path that runs from k to ℓ , then $[X^n]_{k\ell} = 0$.

Hence, applying that for tree matrices the $G_{k\ell}^{(1)}$ are null if $k, \ell \in \partial_1$, we can simplify Eq. (S23) to

$$G_1 = \frac{1}{\begin{pmatrix} 0 & w \\ z & 1 \end{pmatrix} - A_{11} - \sum_{k \in \partial_1} A_{1k} G_k^{(1)} A_{k1}}. \quad (\text{S25})$$

This equation can be generalized to an arbitrary node j because the Schur formula works the same way upon a permutation that is equivalent to relabelling of nodes. Hence, for an arbitrary node $j = 1, \dots, N$, Eq. (S25) becomes

$$G_j = \frac{1}{\begin{pmatrix} 0 & w \\ z & 1 \end{pmatrix} - A_{jj} - \sum_{k \in \partial_j} A_{jk} G_k^{(j)} A_{kj}}. \quad (\text{S26})$$

This set of equations is not closed, because in general $G_j \neq G_j^{(k)}$ for $k \in \partial_j$. To close the equations, we can repeat the same procedure on the N cavity graphs obtained by removing one node at a time. We then obtain

$$G_k^{(j)} = \frac{1}{\begin{pmatrix} 0 & w \\ z & 1 \end{pmatrix} - A_{kk} - \sum_{\ell \in \partial_k \setminus j} A_{k\ell} G_\ell^{(k,j)} A_{\ell k}}, \quad (\text{S27})$$

where $j \in \{1, 2, \dots, N\}$, $k \in \partial_j$, and $G_\ell^{(k,j)}$ are defined analogously to Eq. (S24) but on the graph where the two nodes k, j have been removed.

Note that in general $G_\ell^{(k,j)} \neq G_\ell^{(k)}$, and the recursion has to be continued. However for tree matrices the recursion can be closed at the second step. Indeed, since nodes ℓ and j belong to isolated trees on the cavity graph where node k has been removed, the further removal of node j does not affect $G_\ell^{(k)}$ and therefore $G_\ell^{(k,j)} = G_\ell^{(k)}$. We finally obtain a closed set of equations on a tree

$$G_k^{(j)} = \frac{1}{\begin{pmatrix} 0 & w \\ z & 1 \end{pmatrix} - A_{kk} - \sum_{\ell \in \partial_k \setminus j} A_{k\ell} G_\ell^{(k)} A_{\ell k}}, \quad (\text{S28})$$

for all $k \in \partial_j$.

The Eqs. (S26) and (S28) are the relations (8) and (10) which we aimed to prove.

DERIVATION OF THE RELATIONS (21) AND (22) FOR $S(t)$ IN THE CASE OF BIMODAL DISORDER

The case with the bimodal disorder corresponds to the distribution of diagonal elements $p_D(x) = (1-q)\delta(x+\mu_1) + q\delta(x+\mu_2)$. In order to simplify expressions in this section, we consider a shifted distribution $p'_D(x) = (1-q)\delta(x) + q\delta(x-\mu)$. At the end of the calculations we use the fact that

$$S_{p_D}(t; \mu_1, \mu_2) = e^{-2\mu_1 t} S_{p'_D}(t; \mu = \mu_1 - \mu_2), \quad (\text{S29})$$

which can be easily shown by changing variables $z \rightarrow z - \mu_1$, $w \rightarrow w - \mu_1$ in Eq. (17).

In this case $\int dx p'_D(x) \frac{1}{(z-x)(w-x)} = \frac{1-q}{wz} + \frac{q}{(w-\mu)(z-\mu)}$ and Eq. (17) reads

$$S_{p'_D}(t) = \frac{1}{(2\pi i)^2} \oint_{\gamma} dz dw \frac{e^{t(z+w)}}{\left[\frac{1-q}{wz} + \frac{q}{(w-\mu)(z-\mu)} \right]^{-1} - r^2}. \quad (\text{S30})$$

The integrand can be rewritten using

$$\frac{1}{I^{-1} - r^2} = \frac{I}{1 - r^2 I} = \frac{1}{r^2} \sum_{m \geq 0} (r^2 I)^{m+1}, \quad (\text{S31})$$

yielding

$$S_{p'_D}(t) = \frac{1}{(2\pi i)^2} \sum_{m \geq 0} r^{2m} \oint_{\gamma} dz dw e^{t(z+w)} \left(\frac{1-q}{wz} + \frac{q}{(z-\mu)(w-\mu)} \right)^{m+1}. \quad (\text{S32})$$

Using the binomial theorem, we get

$$S_{p'_D}(t) = \sum_{m \geq 0} r^{2m} \sum_{n=0}^{m+1} \varphi(n, m; q, \mu; t), \quad (\text{S33})$$

where we denoted

$$\varphi(n, m; q, \mu; t) := \binom{m+1}{n} q^n (1-q)^{m+1-n} \left[\frac{1}{2\pi i} \oint_{\gamma} dz \frac{e^{tz}}{z^{m+1-n}(z-\mu)^n} \right]^2. \quad (\text{S34})$$

To compute the contour integral, we need to evaluate the residues at $z = 0$ and $z = \mu$, and sum them up. They read

$$\text{Res} \left[\frac{e^{tz}}{z^{m+1-n}(z-\mu)^n}; z = 0 \right] = \frac{(-1)^n t^m \text{U}(n, m+1, \mu t)}{(m-n)!}, \quad (\text{S35})$$

$$\text{Res} \left[\frac{e^{tz}}{z^{m+1-n}(z-\mu)^n}; z = \mu \right] = \frac{(-1)^{m+1-n} t^m e^{\mu t} \text{U}(m-n+1, m+1, -\mu t)}{(n-1)!}, \quad (\text{S36})$$

where $\text{U}(a, b, z)$ is the Tricomi hypergeometric function (see Eq. (13.2.7) in [7]). Indeed,

$$\text{Res} \left[\frac{e^{tz}}{z^{m+1-n}(z-\mu)^n}; z = 0 \right] = \frac{1}{(m-n)!} \lim_{z \rightarrow 0} \frac{d^{m-n}}{dz^{m-n}} e^{tz} (z-\mu)^{-n}, \quad (\text{S37})$$

which using Leibniz formula for the derivative of a product reads

$$= \frac{1}{(m-n)!} \lim_{z \rightarrow 0} \sum_{s=0}^{m-n} \binom{m-n}{s} \frac{d^{m-n-s}}{dz^{m-n-s}} [e^{tz}] \frac{d^s}{dz^s} [(z-\mu)^{-n}] \quad (\text{S38})$$

$$= \frac{1}{(m-n)!} \lim_{z \rightarrow 0} \sum_{s=0}^{m-n} \binom{m-n}{s} t^{m-n-s} e^{tz} (-n)_s (z-\mu)^{-n-s} \quad (\text{S39})$$

where $(a)^s = \prod_{j=0}^{s-1} (a-j)$ denotes the falling factorial. Taking the limit and rearranging terms, we obtain

$$\text{Res} \left[\frac{e^{tz}}{z^{m+1-n}(z-\mu)^n}; z = 0 \right] = \frac{(-1)^n \mu^{-m} \text{U}(n-m, 1-m, \mu t)}{(m-n)!}. \quad (\text{S40})$$

The use of Kummer's transformation [7, Eq. (13.2.40)] $z^{b-1} \text{U}(a, b, z) = \text{U}(a-b+1, 2-b, z)$ leads to Eq. (S35). Eq. (S36) is obtained using an analogous reasoning.

Now, thanks to the identity [7, Eq. (13.2.41)]

$$\frac{(-1)^{-a}}{\Gamma(b-a)} \text{U}(a, b, z) + \frac{(-1)^{b-a}}{\Gamma(a)} e^z \text{U}(b-a, b, -z) = \frac{{}_1F_1(a; b; z)}{\Gamma(b)}, \quad (\text{S41})$$

the sum of (S35) and (S36) can be simplified as

$$\text{Res} \left[\frac{e^{tz}}{z^{m+1-n}(z-\mu)^n}; z = 0 \right] + \text{Res} \left[\frac{e^{tz}}{z^{m+1-n}(z-\mu)^n}; z = \mu \right] = \frac{t^m {}_1F_1(n; m+1; \mu t)}{m!}, \quad (\text{S42})$$

in terms of a Kummer confluent hypergeometric function (sometimes denoted $M(a; b; z)$, see [7]).

Isolating the $n = 0$ and $n = m + 1$ terms in (S33), we get

$$S_{p'_D}(t) = \sum_{m \geq 0} r^{2m} \left[\varphi(0, m; q, \mu; t) + \varphi(m + 1, m; q, \mu; t) + \sum_{n=1}^m \varphi(n, m; q, \mu; t) \right]. \quad (\text{S43})$$

Using now the explicit forms

$$\varphi(0, m; q, \mu; t) = \frac{(1 - q)^{m+1} t^{2m}}{(m!)^2}, \quad (\text{S44})$$

$$\varphi(m + 1, m; q, \mu; t) = \frac{q^{m+1} t^{2m} e^{2\mu t}}{(m!)^2}, \quad (\text{S45})$$

and performing two further infinite summations (leading to Bessel functions)

$$\sum_{m \geq 0} r^{2m} \frac{(1 - q)^{m+1} t^{2m}}{(m!)^2} = (1 - q) I_0 \left(2rt \sqrt{1 - q} \right), \quad (\text{S46})$$

$$\sum_{m \geq 0} r^{2m} \frac{q^{m+1} t^{2m} e^{2\mu t}}{(m!)^2} = q e^{2\mu t} I_0 \left(2rt \sqrt{q} \right), \quad (\text{S47})$$

we finally get the result in Eqs. (21) and (22) of the main text, upon using Eq. (S29).

-
- [1] B. Collins, and P. Śniady, *Integration with respect to the Haar measure on unitary, orthogonal and symplectic group* Comm. Math Phys. **264**, 773-795 (2006).
 - [2] T. Rogers and I. Pérez Castillo, *Cavity approach to the spectral density of non-Hermitian sparse matrices*, Phys. Rev. E **79**, 012101 (2009).
 - [3] I. Neri and F. L. Metz, *Spectra of sparse non-hermitian random matrices: An analytical solution*, Phys. Rev. Lett. **109**, 030602 (2012).
 - [4] C. Bordenave and M. Lelarge, *Resolvent of large random graphs*, Random Struct. Alg. **37**, 332 (2010).
 - [5] F. L. Metz, I. Neri and T. Rogers, *Spectral Theory of Sparse Non-Hermitian Random Matrices*, Preprint arXiv:1811.10416 - to appear in J. Phys. A: Math. Theor. (2019).
 - [6] M. Mézard and G. Parisi, *The cavity method at zero temperature*, Journal of Statistical Physics **111**, 1-34 (2003).
 - [7] Digital Library of Mathematical Functions *Confluent Hypergeometric Functions* <https://dlmf.nist.gov/13.2>